Thermal, Mechanical, Dielectric and Morphological Study of Dielectric Filler Based Thermoplastic Nano-Composites for Smart Applications

Anup Poudel[1], Philip Walsh[1], James Kennedy[2], Ken Thomas[1], John G. Lyons[2] and Austin Coffey[1]

[1] Convergent Technology Research Group (CTRG), Department of Engineering Technology, Waterford Institute of Technology (WIT), Cork Road, Waterford, Ireland

[2] Applied Polymer Technology, Athlone Institute of Technology (AIT), Athlone, Ireland

Corresponding author:

a. Anup Poudel (email: apoudel@wit.ie) - all stages of refereeing and publication

b. Austin Coffey (email: acoffey@wit.ie) -Post-publication

Abstract— Dielectric nanocomposite elastomers based on Poly(styrene-ethylene/butylene-styrene) [SEBS] and Poly(styrene-ethylene/butylene-styrene)-grafted-maleic anhydride [SEBS-g-MA] with barium titanate (BT), suitable for electroactive smart applications were manufactured by using a co-rotating twin screw–extrusion system. The thermal, mechanical, dielectric and morphological effects of additives on SEBS and SEBS-g-MA were investigated. A relative change in dielectric permittivity (33.33 % and -1.5% on SEBS-g-MA and SEBS respectively upon addition 10% of BT) as well as changes in thermal (enthalpy relaxation and thermal transitions) and mechanical (Young's Modulus, hysteresis loss under multiple stress cycles, storage modulus, loss modulus and tan delta) properties of elastomers were found to be a function of additive concentration, compatibility and interaction between elastomers and additive type, orientation of additives and reinforcing factors of additives in elastomers. A simple and effective modeling technique was used to demonstrate the effects on dielectric properties of nanocomposites due to poor dispersion of additives.

Keywords- SEBS, SEBS-g-MA, Dielectric Thermoplastic Elastomers, Dielectric Composites,

Comment [SL1]: Clarify this. You use a dual extrusion system (i.e 2 extruders) and twin screw extruders.

1 Introduction

Dielectric thermoplastic elastomers are thermoplastic polymers which are rubbery in nature with thermoplastic processability and demonstrate mechanical responses when placed in an electric field [1-4]. Different thermoplastic copolymers are available based on styrene block copolymers, co-polyester, polyurethanes, and co-polyamide. Thermoplastic elastomers are formed by blending rubber and thermoplastic polymers, where thermoplastic polymers and rubbers exist in different phases [5, 6]. Poly(styrene-ethylene/butylene-styrene) (SEBS) triblock is a type of styrene block copolymer which consists of polystyrene as end hard blocks and ethylene-butylene as the mid-soft block. Synthesis of SEBS triblock is done by the hydrogenation of double bonds present in poly (styrene- butadiene- styrene) [SBS] triblock. SEBS has become more and more attractive to engineers and scientific communities not only because of its high chemical, weather and heat resistance [7] but also because of electroactive properties [8]. Because of these unique characteristics, it has a huge potential for applications in strain and stress sensing, actuation, and energy generators. Moreover, the attachment of the polar group maleic anhydride on SEBS's carbon backbone provides better dispersion of highly polarizable additives like BT for the enhancement of its electrical property. However, electroactive properties such as actuation, Maxwell stress, polarizing capability and strain sensing abilities of these virgin elastomers and their nanocomposites are dependent on several mechanical, thermal and electrical properties of thermoplastic elastomers. In addition, the type of additives used, dispersion levels and the interaction between elastomers and additives are also of major concern [4-6, 9-13].Elastomers tend to have high dielectric constant under relaxed conditions than stretch conditions [14]. The relative change in polarization under different strain conditions gives high prospect for the use of these elastomers as energy generators, only if these elastomers remain highly mechanically compliant. Moreover, these dielectric thermoplastic elastomers need to have a high dielectric permittivity and high mechanical compliance with very low dielectric loss when used for electroactive applications

Compared to different piezoelectric, shape memory and conventional dielectric polymers used in similar applications, styrene based triblock SEBS was found to have higher electrical elongation (47% versus 0.1% for PZT), higher energy density (139 KJ/m^3 versus 2.5 KJ/m^3 for PZT) and better electromechanical coupling efficiency (0.85 versus 0.6 for PZT) [11, 15, 16]. In addition to its elastomeric properties, SEBS can be easily be processed for its mechanical and electrical performance enhancement. Even though conventional dielectric elastomers such as silicone also have good electromechanical performance [10, 17], several problems such as the requirement of high biased voltage and difficult processing requirements remain unresolved [11, 18]. The

ease of processing of thermoplastic elastomers with the addition of different filler types to tailor their dielectric properties makes them more suitable for artificial muscles, capacitive sensors and capacitive energy harvesters [11, 19].Conductive fillers tend to change the dielectric permittivity of polymer matrices by several folds [20]. He and Tjong [21] reported the dielectric permittivity of PVDF increased by 15 times with the addition 0.5% of reduced graphene sheets. However, they also tend to increase the dielectric permittivity loss of nanocomposites leading such manufactured nanocomposites to have low dielectric strength [22]. In addition, Kim [23] noticed the low deformation on the application of an electric field even at a higher percentage of carbon black. This may be due to a higher relative stiffness change on the polymer nanocomposite matrix, rather than its relative dielectric permittivity increase due to the high reinforcing effect of carbon black. In addition, the high dielectric loss, low dielectric strength, and high reinforcing effects of conductive fillers such as carbon black and graphene limit the applications of elastomers nano-composites for many electroactive applications like energy harvesting and charge storing flexible supercapacitors.

This paper presents the enhancement of dielectric permittivity with very low dielectric loss and minimum increase in stiffness of thermoplastic elastomers using high dielectric fillers based on barium titanate (BT). The aim of ~~this paper~~the current work is to show the importance of compatibility and interaction between additives and polymer matrix to change the dielectric as well as mechanical – properties of these polymers with differring~~ent~~ ratios of nano-additives. Specifically, this paper address following ~~issues~~ (i) the effect of polymer- additives interaction on the electrical, mechanical, thermal and morphological properties of BT/polymer composites (ii) the dielectric and thermo-mechanical response of BT/polymer composites over the range of frequency and temperature respectively (iii) the thermal response of BT/polymer composites (iv) the effect on dielectric properties of BT/polymer composites due to the dispersion of additives in polymer matrix and (v) manufacturing of high dielectric thermoplastic elastomers composites using faster and more cost effective,.simple production processes such as hot melt extrusion in place of conventional solvent methods.~~; which are faster and more cost effective.~~

2 Experimental

2.1 Materials

Poly(Styrene-ethylene/butylene-styrene) [i.e. SEBS triblock] (KRATON® G1652 E Polymer) with linear structure and 29-30% styrene content and Poly(styrene-ethylene/butylene-styrene)-grafted- maleic anhydride [i.e. SEBS-g-MA triblock] (KRATON® FG1901G Polymer) with linear structure and 29-30% styrene content

were obtained from Kraton polymer research, Belgium. High dielectric material BT (100 nm, 99.9%) was obtained from IoLiTec Ionic Liquids Technologies GmbH, Germany.

2.2 Preparation of Nanocomposites

Material blending was carried out in a corotating twin screw extruder (extruder 1) with L/D ratio of 25:1. Samples of SEBS and SEBS-g-MA with different percentages of BT (1%, 5%, and 10%) were subsequently produced. Extrusion was carried out at a screw speed of 70 revs/min, torque between 15 to 10 Nm, die pressure between 5 to 10 Psi and temperature profile as per Table 1~~Table 1~~.

Comment [SL2]: Torque reading and head pressure are really results rather than process settings. (you cant set the torque or die head pressure it results from the viscosity of the polymer + Shear + temp profile)

Table 1 Temperature profile of SEBS and SEBS-g-MA composite (extruder 1)

Materials	Temperature Profile (Zones) (^{o}C)					
	1	2	3	4	5	Die
SEBS Composites	32	176	220	240	240	240
SEBS-g-MA Composites	30	160	190	200	200	200

The extruded material from extruder 1 was pelletized and fed using gravimetric feeder into a separate corotating twin screw extrusion machine (extruder 2) of L/D of 25:1. The extrudate was then passed through a roller system running at a constant speed of 0.5rev/min in order to produce a constant thickness sheet. Processing was carried out with a screw speed of 70 revs/min, torque between 25 to 140 Nm, die pressure between 4-7 Psi and temperature profile listed as per Table 2~~Table 2~~.

Comment [SL3]: Temp of roller system?

Comment [SL4]: As above

Table 2 Temperature profile for SEBS and SEBS-g-MA composite (extruder 2)

Materials	Temperature Profile (Zones) (°C)						
	1	2	3	4	5	6	Die
SEBS Composites	30	100	180	220	240	245	245
SEBS-g-MA Composites	140	155	170	180	180	190	200

2.3 Dielectric Characterization

Dielectric characterization of flat samples of each composite of thickness values between 1-2 mm was carried out using a Solatron 1260 impedance analyzer with a 1296 dielectric interface. In addition, a Solatron 1296 2A sample holder was used to facilitate measurement of the solid samples; which consisted of two parallel electrodes, both of 40 mm diameter, between which the material was placed and a 3Vrms alternating voltage

applied. Each sample was measured five times and the standard deviation was found to be less than 0.1% of all sample types.

Comment [SL5]: Was there a consistent stand down time between production of parts and measurement (variances in shrinkage or crystallinity over time may change results)

2.4 Mechanical Characterization

Five ASTM Type I tensile bars were obtained for each composite by cutting an extruded sheet of each sample along the axis of screw rotation obtained from the extrudate. Tensile testing was carried out using Zwick/ Roell Z010 with 2.5 KN load cell capacity. The speed and the maximum extension between the grips were maintained at a speed of 500mm/min and 200% respectively. Finally, the average curve of five samples was calculated and plotted for each composite type. Then, standard Young's modulus of elasticity was measured for each composite at different strain point. Similarly, cyclic testing was performed on all composites samples. Total hysteresis loss and total elastic energy present were measured using work curves for each cycle. The total amount of energy required for composite to extend by 200% was divided into two types of energy; (i) elastic energy and (ii) loss energy as shown in Figure 1~~Figure 1~~ .

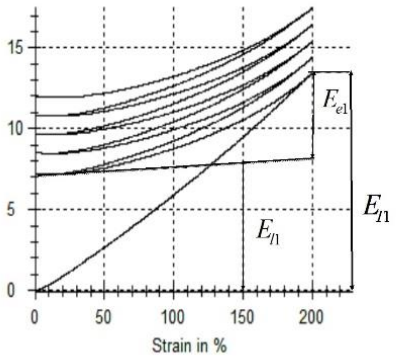

Figure 1 Total energy (E_{T1}) divided into elastic energy (E_{el}) and loss energy (E_{l1}) for cycle 1 for SEBS

$$E_{Ti} = E_{ei} + E_{li} \qquad (1)$$

Where, E_{Ti}, E_{ei} and E_{li} are total energy applied, elastic energy present in the material after reloading and loss energy or hysteresis loss of thermoplastic elastomer respectively for the cycle i.

The term loss factor was used to measure the shape memory properties of nanocomposites under large extension. The loss factor can be directly defined as

$$LF_i = E_{li} / E_{ei} \qquad (2)$$

2.5 Dynamic mechanical analysis

Tensile flat samples were prepared by cutting an extruded sheet along the axis of screw rotation obtained from co-rotating, twin screw extrusion. Dynamic mechanical analysis was carried out on a TA Instruments DMA 800 to evaluate the viscoelastic properties of SEBS elastomer. The experiment was carried out in a ramp temp/multi-frequency mode from 25 to 140^{o}C at a frequency of 1 Hz with a heating rate of 3 °C/min. DMA was used to measure transitions of mechanical failure of elastomer, maximum molecular chain movements of the same and glass transition of styrene block of a sample using data obtained from storage modulus, loss modulus, and tan delta, respectively, as the sample deformed at an amplitude of 16 µm under a sinusoidal deformation of 1Hz.

2.6 Modulated Differential Scanning Calorimetry (MDSC)

MDSC of all composites were carried with TA instrument 2000 MDSC. The heat capacity was calibrated using sapphire, while temperature and baseline were calibrated using indium. An oscillation period of 60 seconds and amplitude of ±0.47°C was used in modulated heating and cooling experiments. SEBS was subjected to equilibration from 22 to –80ºC followed by heating at 3°C/min to 180ºC. At the beginning and end of each heating and cooling run, materials were held isothermally for 3 min to obtain thermal stabilization between the reference pan and sample pan. TA software for MDSC was used for recording, analysis and deconvolution of the signals. The least square method was used to smooth all the curves for better analysis. The level of smoothing was selected within the range of 3 ºC to give minimum distortion and no shift of peaks. Thermal analysis of each composite type was performed using total heat flow curve and derivative of reversible specific heat capacity curve. The temperature derivative of reversible specific heat capacity was used to measured glass transition because it is reported to show high sensitivity to the process of heat flow during glass transition [24, 25].

2.7 Attenuated Total Reflectance -Fourier Transfer Infrared Spectroscopy (ATR- FTIR) studies

Polymer- additive interaction in the different composites was studied using ATR-FTIR. Infrared spectra of all composites were obtained with a VARIAN 600 ATR-FTIR. ATR-FTIR spectroscopy was carried out at room temperature on clean solid extruded flat samples with a resolution of 4 cm^{-1}. All data were collected between 600 cm^{-1} and 4000 cm^{-1} with an average of 32 scans.

2.8 Morphological Studies

Four samples (SEBS, SEBS-g-MA, SEBS with 10% of BT and SEBS-g-MA with 10% of BT) were chosen for morphological analysis. Samples were submerged in liquid nitrogen and were ~~broken~~ cryofractured to visualize the distribution of additives in polymer matrix along the thickness (traverse cross section area). Morphological studies of prepared samples were carried out with TESCAN (Electron Scanning Microscopy) at 20 KV. Different regions were selected and element mapping was performed to access the materials distribution profile.

Comment [SL6]: I assume these samples were gold coated? Should that be noted here?

You mention element mapping later on but there is no mention of that in the experimental – add EDX here?

3 Results and Discussion

The dielectric permittivity calculated for SEBS and SEBS-g-MA composites from the Salotron 1296 at a frequency of 1 KHz at room temperature is shown Table 3.

Table 3 Dielectric permittivity of SEBS and SEBS-g-MA with BT

Additives	Real dielectric constant of nanocomposite at 1 KHz (ε_r) with percentage changed with additives	
	SEBS's ε_r (% change)	SEBS-g-MA's ε_r (% change)
Virgin	3.18	3.79
BT-1%	3.56 (11.69)	4.49 (18.6)
BT -5%	4.07 (27.68)	4.68 (19.6)
BT-10%	3.15 (-1.2)	5.03 (32.8)

The graph for the real dielectric permittivity of SEBS and SEBS-g-MA composites is shown in Figure 2~~Figure 2~~.

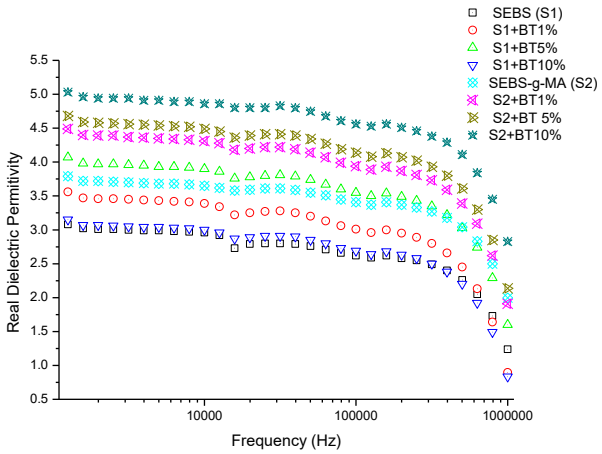

Figure 2 Real component of dielectric permittivity of SEBS (S1) and SEBS-g-MA (S2) composite with different percentages of BT

The dielectric loss (tan delta) was also measured and found to be less than 0.01 below 1KHz of all composite samples. However, the loss was found to increase with an increase in frequency.

As is self-evident, BT tends to improve the dielectric permittivity of the polymer matrix to some threshold as predicted by in the literature[26]. Orientation shape and dispersion of additives in the polymer matrix defines the resultant dielectric developed the nanocomposite [27]. On addition of high dielectric permittivity materials (such as BT), the interfacial polarization occurs between the polymer matrix and additives particles resulting in enhancement of dielectric permittivity of dielectric nanocomposites [28-31].

In Figure 2~~Figure 2~~ and Table 3, it is observed that the increase in dielectric permittivity of SEBS with highly polar dielectric fillers like BT occurs up to a certain percentage (typ. 5%). Even though the permittivity of SEBS with high percentages is expected to increase with increased amounts of BT, the permittivity of the materials at high percentages of BT (10%) show a decrease in relative dielectric permittivity. This decrease in the dielectric permittivity of the polymer for increased dielectric filler content is very peculiar, as it directly ignores the concept, that relative permittivity should increase with higher concentrations of dielectric fillers as a result of the influence of particle distribution, polarization and interfacial polarization between the filler and the polymer matrix. However, this type of effect is also found in different epoxy composites by Patsidis et al [32] and Zhang et al. [24]. This negative change in dielectric permittivity is not observed when the compatibility is increased between SEBS and BT by attachment of polarizing molecule maleic anhydride (MA) as shown in Figure 2~~Figure 2~~. Similarly, Stoyanov[7], and Yang and Kofinas[33] also found that the dielectric permittivity increased with an increase in TiO_2 content making SEBS compatible to the additives. This result shows the role

of the interaction between additives and polymer molecule for the enhancement of dielectric permittivity. The increase in dielectric permittivity with low dielectric loss optimizes the electroactive properties of different elastomers thereby increasing the potential of these elastomers to be used for strain/stress sensors, capacitive energy generators, artificial muscles and flexible charge storing capacitors.

The enhanced dielectric permittivity of elastomers composites is a crucial factor for an electroactive applications. Mechanical properties (such as Young's modulus and loss factor) and viscoelastic properties are also equally important to determine stiffness, flexibility, hysteresis loss and stability of such composites during their uses

Figure 3~~Figure 3~~ and Figure 4~~Figure 4~~ show the tensile profile of SEBS and SEBS-g-MA with BT respectively. The stress was measured up to 200 % strain for all samples. All samples of both composites were found to be highly elastic with no breakage till the measured elongation. In both composite types, curves consist of a linear region or an elastic region, a necking point, a drawing region and again a linear region at all concentration of modifiers. The stretching of the necking region also known as natural draw ratio is hardly seen in both composite types, but it prevails in most experiments as it is a function of temperature and processing parameters [34]. Unlike most of the plastic materials, thermoplastic elastomers continue to extend linearly after necking of tensile samples and still possess elastic property. It is because of the fact that the necking produces stronger microstructure leading to the higher amount of energy or stress required for breakage [34].

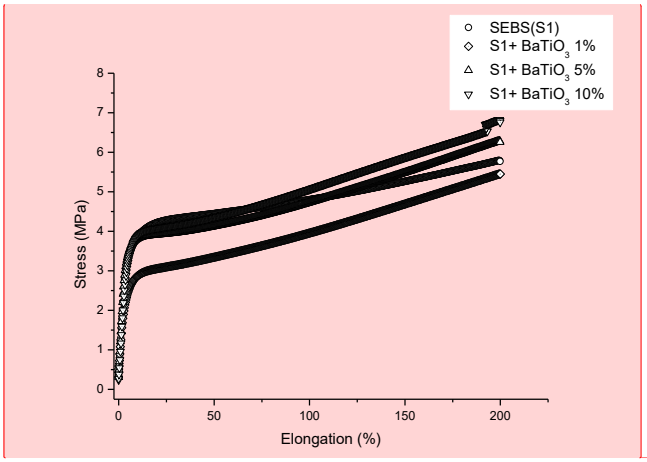

Figure 3 Tensile properties of SEBS with BT

Comment [SL7]: These graphs could do with some color or different symbols – very difficult for reader to interpret at this size. Bar chart later works well but this is difficult

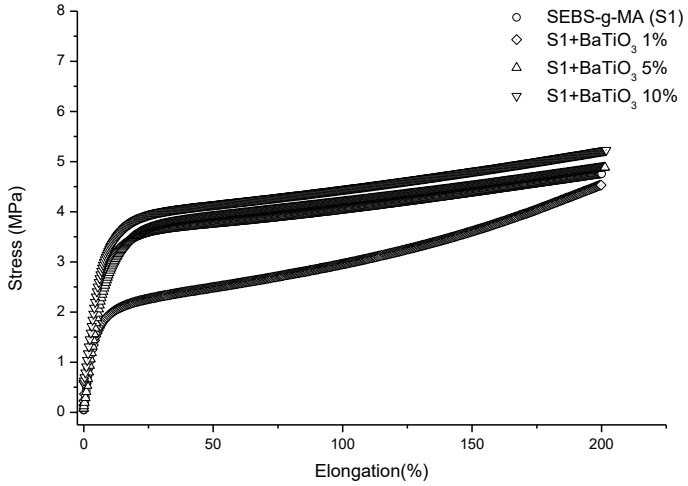

Figure 4 Tensile properties of SEBS-g-MA with BT

The modulus of resilience is defined as energy absorbed by the material below its yield point. Not much difference in resilience was observed with the addition of 5% and 10% BT, however, the modulus of resilience was found to decrease upon addition of 1% of BT for both polymer matrices. The decrease in modulus of resilience at low concentration of BT can be defined based on the orientation of additives. The orientation of BT additives is not along the direction to the axis of screw speed at which tensile measurement of the extrudate was taken, However, at a high percentage of BT, the mechanical interlocking effects of additives are also seen along the tensile measurement axis giving almost the same modulus of resilience. The energy observed between yield point and breakage defines the modulus of toughness of the material. From Figure 3~~Figure 3~~, the addition of 5% and 10% BT increases the modulus of toughness of SEBS, but not in the same fashion as 5% and 10% of BT in SEBS-g-MA as shown in Figure 4~~Figure 4~~. SEBS at all concentrations of BT show low values of stress to strain ratio even at 50% strain than a virgin SEBS suggests a higher drawing region which may be due to lack of reinforcement and low compatibility of SEBS with BT as shown in Table 4~~Table 4~~, but his effect is not observed in SEBS-g-MA. However, SEBS and SEBS-g-MA with 1% of BT show a low toughness compared to pure SEBS and SEBS-g-MA respectively, but this result might be altered if the material is extended to the breaking point as the slope gradient of SEBS as well as SEBS-g-MA with 1% of BT is higher after the yield point of virgin SEBS and SEBS-g-MA respectively which can be seen from Table 4~~Table 4~~. The percentage

change in Young's modulus of SEBS with 1% of BT with respect to unfilled SEBS was found to change significantly from -23.9% to -11.4% when measured at 50% of strain and 150 % strain respectively.

Table 4 Young's modulus of nanocomposites with different percentage of BT

Materials	Secant Young's modulus of nanocomposite different strain (MPa)			
	1% (% Δ)	50% (% Δ)	100% (% Δ)	150% (% Δ)
SEBS (S1)	110.0	8.8	4.8	3.5
S1 + BT 1%	100.0 (-9.1)	6.7 (-23.9)	3.9 (-18.8)	3.1(-11.4)
S1 + BT 5%	116.0 (5.4)	8.2 (-6.8)	4.7 (-2.0)	3.6 (2.8)
S1 + BT 10%	95.1 (-13.4)	8.7 (-1.1)	5.0 (4.2)	3.9 (11.4)
SEBS-g-MA (S2)	45.0	7.5	4.0	2.9
S2 + BT 1%	47.0 (4)	5.0 (-33.3)	3.0 (-25.0)	2.4 (-17.24)
S2 + BT 5%	40.0 (-11.1)	7.6 (1.3)	4.1 (0.25)	3.0 (3.4)
S2 + BT 10%	47.4 (4)	8.2 (9.3)	4.4 (10)	3.2 (10.34)

~~.~~Not much effect is ~~seen~~ observed in Young's modulus with the addition of additives to elastomers to 1% strain, but the modulus of SEBS and SEBS-g-MA increases with the increase of BT percentage at the higher extension. Unlike SEBS-g-MA composite, low values of stress to strain ratio of - SEBS at all concentrations of BT at 50% strain compared to pure SEBS suggests a higher drawing region which may be due to lack of reinforcement and low compatibility of SEBS with BT. This result also suggests poor miscibility of BT on SEBS when using the current processing configuration described. Generally, manufacturing of highly flexible dielectric composites has huge potential for electroactive applications. However, the incompatibility between additive and elastomer leads to poor mechanical and electrical performance.

Figure 5~~Figure 5~~ shows the loss factor of different composites under each cycle. According to Cantournet et al.[35], the extension of elastomers occurs due to sliding (after the elastic limit) and non-sliding action (within elastic limit in the first cycle) between hard and soft blocks. This condition is also observed during the unloading condition. The loss of stiffness during cyclic testing after the first cycle results in stress softness behavior[35] leading to a low loss in consecutive cycles as shown in Figure 5~~Figure 5~~. This stress hysteresis or stress softening behavior was first described by Mullins and is known as Mullin's effect [36]. Due to stress softening effect of dielectric thermoplastic elastomers nanocomposites, the loss factor drastically decreases

Formatted: Font color: Black

Formatted: Font color: Black

from first to the second cycle. Upon addition of 1% of BT, the loss factor is highly increased in all cycle due to high mechanical interlocking. However, this effect was hindered as the percentage of BT was increased due to the formation of agglomerations. In SEBS with 10% BT, the loss factor was found to be lower than virgin SEBS almost for all cycle. It is because of lack of interaction between BT and SEBS and agglomeration of BT in SEBS during the manufacturing procedure. Although this result seems better for electroactive applications, agglomeration of BT hinders overall polarization effects of composites as well as makes mechanically unstable with time.However, SEBS-g-MA shows improved interaction with BT leading to the better dispersion of BT and a continuous loss factor at all concentrations due to the presence of the polar MA molecule.

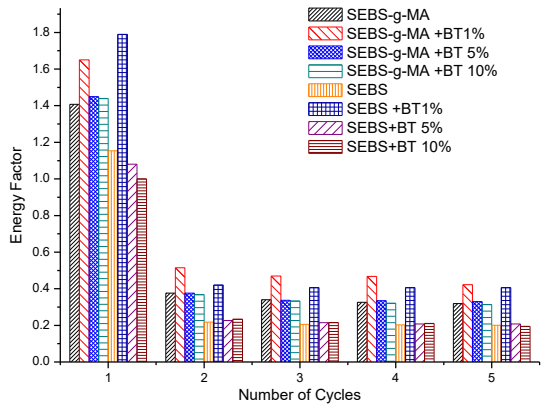

Figure 5 Loss factor for each cycle of different composites presented with different colors

Table 5~~Table 5~~ shows storage modulus, loss modulus and tan delta of SEB and SEBS-g-MA with BT measured at a test frequency of 1Hz and 31^{o}C temperature in transverse and parallel direction to the axis of screw rotation.

Formatted: Font: Not Bold

Table 5 Storage modulus (G'), Loss modulus (G'') and Tan delta of nanocomposites measured at a test frequency of 1 Hz and 31 ^{o}C temperature

Materials	In transverse direction to extrusion			In parallel direction to extrusion		
	G'	G''	Tan Delta	G'	G''	Tan Delta
	MPa (% Δ)	MPa (% Δ)	NA (% Δ)	MPa (% Δ)	MPa (% Δ)	NA (% Δ)

SEBS (S1)	5.16	0.20	0.039	104.27	5.19	0.049
S1+ BT -1%	7.65 (38.7)	0.64 (220.0)	0.084 (115.0)	98.29 (-5.7)	8.15 (57.0)	0.083 (69.0)
S1+BT -5%	8.94 (73.2)	0.38 (180.0)	0.043 (10.25)	71.39 (-31.5)	4.03(-22.3)	0.056 (14.3)
S1+BT-10%	5.84(13.2)	0.24 (20.0)	0.040 (2.5)	75.65 (-27.4)	3.93(-24.3)	0.051 (4.1)
SEBS-g-MA (S2)	4.12	0.39	0.095	70.70	6.34	0.047
S2+ BT-1%	12.14(94.7)	1.10(182.1)	0.090 (-5.0)	36.27(-48.6)	3.12(-50.8)	0.086 (74.4)
S2+BT-5%	4.60(11.7)	0.42 (7.7)	0.091(-4.2)	56.86 (-19.5)	4.65(-26.7)	0.082 (85.1)
S2+BT-10%	4.57 (10.9)	0.41 (5.1)	0.091(-4.21)	44.05 (-37.6)	3.906(-8.4)	0.089 (89.3)

In the transverse direction of the extrusion, BT showed an increase in moduli and tan delta in both SEBS and SEBS-g-MA-based nanocomposites.

Unlike the high increase in storage modulus and loss modulus observed in the transverse direction, the addition of BT was found to decrease the loss moduli of the nanocomposites in the parallel direction; except for low % weight of nanofiller (SEBS with 1% BT). The decrease with both moduli observed is due to the presence of low shear stress along the axis of screw rotation during extrusion, however, the reinforcing effect increases with an increase in the amount of BT with SEBS. In addition, the decrease in the value of tan delta of SEBS-g-MA was observed in a transverse direction with the addition of BT fillers. However, this effect was not observed in SEBS composites. This result also suggests higher compatibility and dispersion of BT fillers with SEBS-g-MA matrix compared to SEBS matrix. Compatibility between a filler and a polymer matrix is a crucial parameter for sustainable electrical and mechanical property for an electroactive application.

Generally, with the addition of additives to elastomers, they tend to change the stiffness of the material at higher temperatures when they are measured at low strain conditions using DMA. However, the addition of BT did not improve the storage modulus of SEBS at high temperature as shown in Figure 6~~Figure 6~~. In addition to this, the molecular motion of SEBS starting around 40 °C rise in a similar fashion to higher temperature till 90 °C upon addition of a different percentage of BT shown in Figure 7~~Figure 7~~. Moreover, the peak of tan delta also remains almost constant at all concentrations of BT as shown in Figure 8~~Figure 8~~.This suggests very less interaction or no interaction between non-polar SEBS with highly polar BT dielectric filler.

Wang [37] used a concept of surface energy to describe the dispersion of additives in a rubber matrix either in the form of aggregates or agglomerates. He used a kinetic model as described by equation (3).

$$\Delta w = w_{aa} + w_{pp} - 2w_{ap} \qquad (3)$$

Where Δw is the change in adhesion energy, w_{aa} is the adhesive energy between additive-additive particles, w_{pp} is the adhesive energy between the polymer-polymer molecule and w_{ap} is the adhesion energy between additive and polymer. According to the Wang's model, when Δw=0, additives, once dispersed, they don't form agglomerates. If Δw>0, the aggregates forms agglomerates once they are totally dispersed in thermoplastic elastomers. Finally, if Δw<0, the aggregates have a high tendency to disperse in the polymer matrix[38].

According to Wang equation, the value of Δw should be either equal to 0 or greater than 0 when BT is dispersed into SEBS matrix leading to poor dispersion ability. A better manufacturing procedure (such as the use of supercritical CO_2 assisted extrusion) allowing better dispersion of additives into polymers can sometimes readily solve the issue faced in this context [39-42]. If the Δw is positive and high enough, other techniques like a molecular modification of SEBS (such as the attachment of maleic anhydride with SEBS) will lead to the better dispersion ability of BT in the polymer.

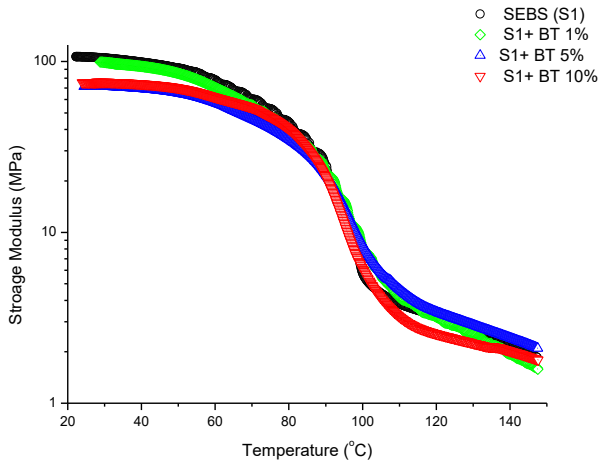

Figure 6 Storage modulus of SEBS (S1)/BT composites presented with different colors

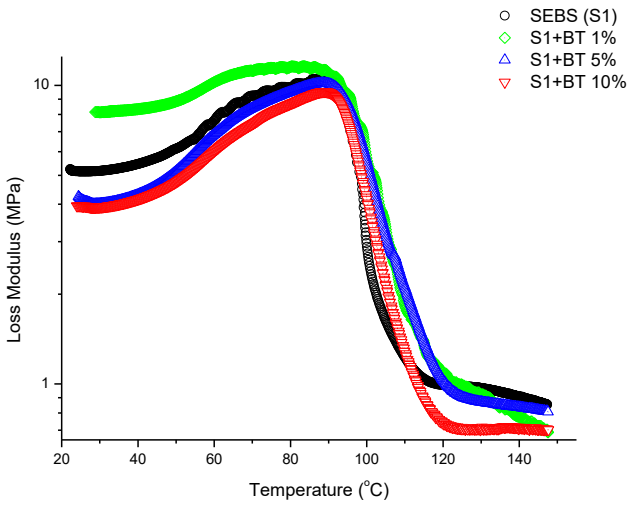

Figure 7 Loss modulus of SEBS (S1)/BT composites presented with different colors

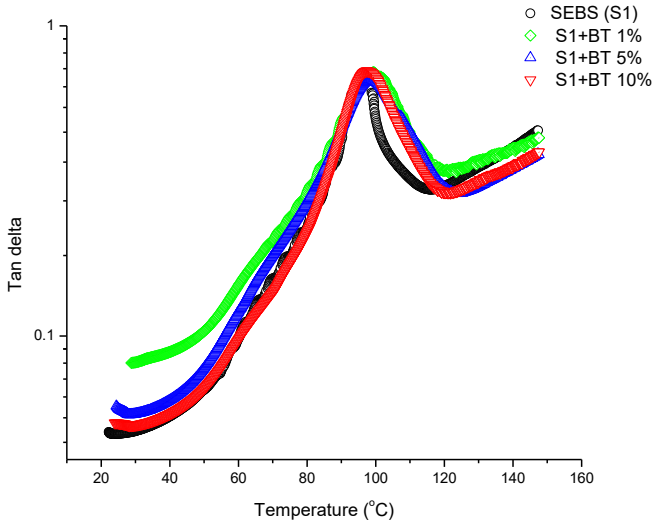

Figure 8 Tan delta of SEBS (S1)/BT composites presented with different colors

The SEBS-g-MA- BT composites show different behavior compared to SEBS-BT composites based on the storage modulus, loss modulus, and tan delta. Figure 9~~Figure 9~~ shows the storage modulus of SEBS-g-MA- BT nanocomposites. The stability or elastic property of SEBS-g-MA- BT nanocomposite increases with an increase in BT content at a higher temperature making it more thermal resistive. Loss modulus shows a high increase in the width of the peak of loss modulus with an increase in BT. Generally, a broad peak of loss modulus represents the higher damping behavior of the material[43]. However, in the case of Figure 10~~Figure 10~~, a broad

peak is not due to the higher molecular motion between two segments rather it is because of resistance to molecular movement of between segments at higher temperatures due to the high interaction between polar MA molecule of SEBS-g-MA and highly polar dielectric filler BT. Due to the reinforcing nature and high interaction of compatible BT additives, molecules of SEBS-g-MA show only low molecular movement at higher temperature thereby lowering the loss modulus value when measured using DMA under low strain condition. Because of a hindrance in molecular movement at a higher temperature when measured at low strain conditions in DMA, the peak appears to be broad rather than a narrow peak. SEBS-g-MA/BT composites show a broader peak compared to virgin SEBS-g-MA as shown in Figure 11~~Figure 11~~. In addition, Figure 11~~Figure 11~~ also shows a low value of tan delta with the addition of BT fillers at all range of the measured temperatures. This result also suggests the material is still a low loss material although the amount of BT was increased. A temperature shift in the peak of the tan delta was observed on SEBS-g-MA upon addition of BT. This effect ~~was~~ is likely due to an absolute change in storage and loss modulus under low strain conditions as shown in Figure 9~~Figure 9~~ and Figure 10~~Figure 10~~. Some authors suggest that these changes observed on the tan delta transition peaks are due to the addition of additives [44], whereas some suggest a change in time-dependent relaxation of polymers molecules due to the effect of additives[45].

Comment [SL8]: 'was' is a bit too definitive here. 'Is likely due to' or 'the authors believe' may be more appropriate

The temperature shift in the peak of the tan delta was found to be directly proportional to the amount of BT contents since when the amount of filler is sufficient, additives form a higher reinforcing effect, thereby overcoming the hydrodynamic effects of polymers. However, this network can be broken down at a high percentage of strain (generally above 0.1% strain range) which is best defined by the Payne effect [38, 46-48]. This effect is not seen when strain % is very low as used in this work. The shift in tan delta (a representation of glass transition of hard block) is an essential parameter to study for different nanocomposites as it defines mechanical stability as well as viscoelastic properties of nanocomposites for their all possible applications under different strain/ stress condition for different applications.

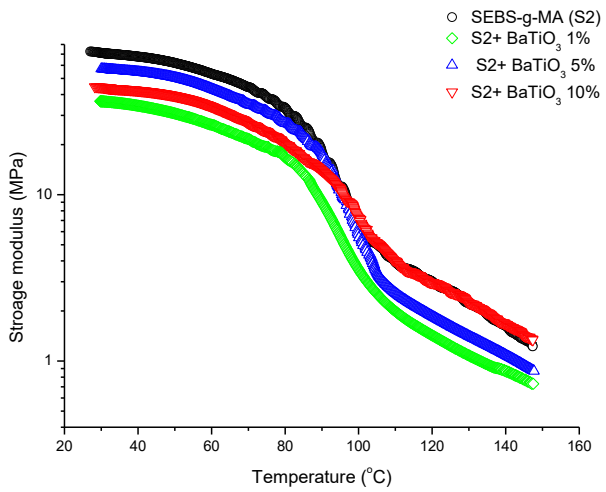

Figure 9 Storage modulus of SEBS-g-MA (S2)/BT composites presented with different colors

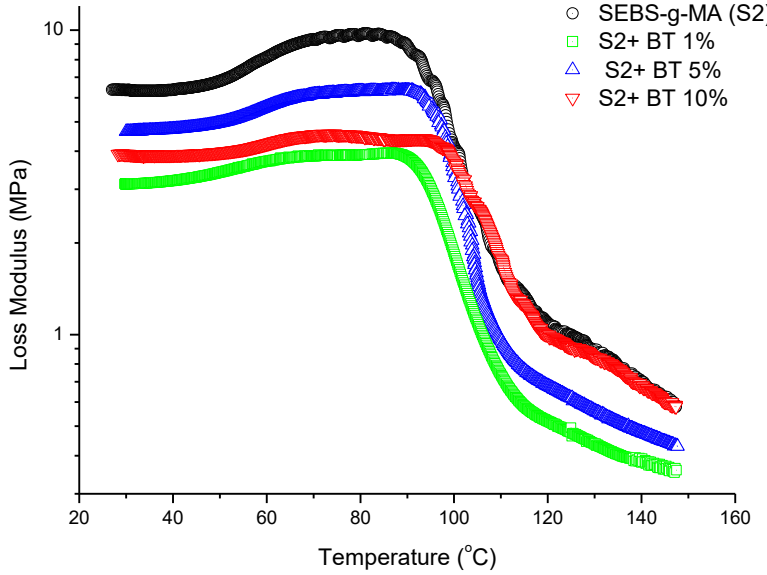

Figure 10 Loss Modulus of SEBS-g-MA (S2)/BT composites presented with different colors

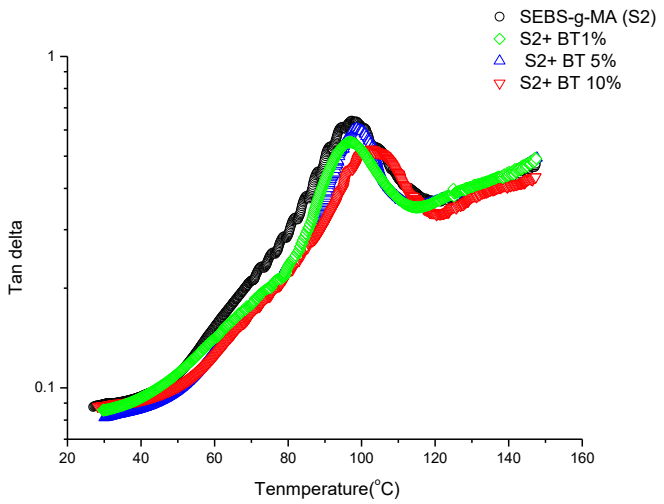

Figure 11 Tan delta of SEBS-g-MA (S2)/BT composites presented with different colors

Figure 12 and Figure 13 shows the heat flow curve, and temperature derivative of reversible specific heat capacity respectively for different BT/ polymer matrices. Although the peak of total heat enthalpy around 11 °C was not highly altered upon addition of BT on both triblock, rearrangement of this peak due to densification of aromatic structure (T_{C1} and T_{C2} in Figure 12 and Figure 13 respectively) forming multiple interphases with soft block soon after the endothermic peak enthalpy was found to be affected upon addition of BT. This effect is more prominent in SEBS-g-MA than SEBS triblock due to the high interaction of the polar MA molecule attached to the soft block with BT. Similarly, the rate of change of heat enthalpy soon after glass transition (measured in Figure 13) in SEBS-g-MA also showed significant change upon addition of BT than in SEBS as shown in Figure 12. However, the glass transition temperature of different composites (ca. -53°C for SEBS-g-MA composites and -56°C for SEBS composites) calculated by temperature derivative of reversible specific heat capacity were found almost to be constant with the addition of a different amount of BT additives. A slight different in the glass transition of the soft block was observed between SEBS-g-MA and SEBS triblock because of the presence of MA, a bulkier molecule, in an ethylene/butylene molecule in SEBS-g-MA.

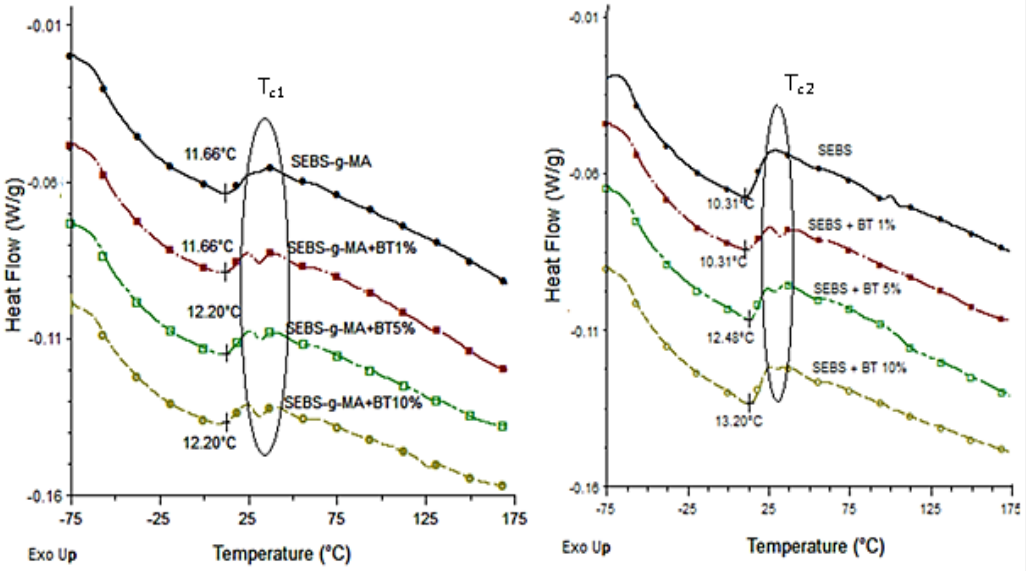

Figure 12 Total heat flow curve of SEBS-g-MA/ BT composites (left) and SEBS/BT composites (right)

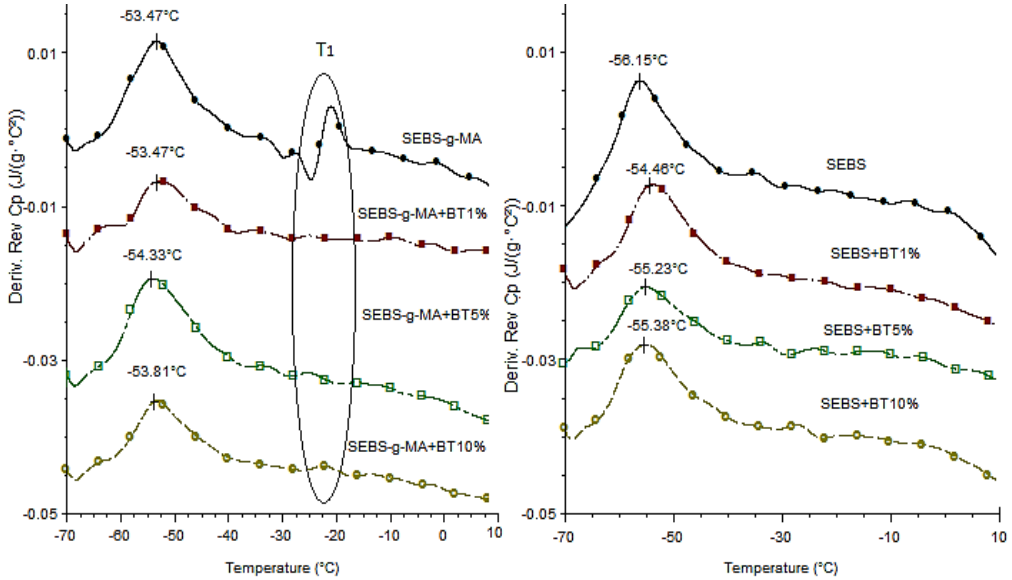

Figure 13 Temperature derivative curve of reversible Cp curve of SEBS-g-MA/ BT composites (left) and SEBS/BT composites (right)

Moreover, the broadening of Tg (ca. 53℃) in SEBS-g-MA compared to SEBS upon addition of BT also confirms the formation of homogenous mixtures of SEBS-g-MA/BT composites than SEBS/BT composites. Also, there is a sudden change around -25 ℃ in SEBS-g-MA as shown in Figure 12 and Figure 13 (T1). This sudden change observed was found being altered upon addition of BT additives. It also confirms an interaction of SEBS-g-MA triblock with BT additives.

Figure 14 and Table 6 shows the ATR-FTIR graphs of SEBS and SEBS-g-MA triblock and different frequencies of bands observed in FTIR spectra of the studied SEBS and SEBS-g-MA polymers respectively [49-52]. Generally, anhydride shows two FTIR bands due to vibration coupling of C=O groups. In succinic anhydride, these two bands are seen at 1871 cm^{-1} and 1793 cm^{-1} for asymmetric and symmetric vibration of C=O groups respectively [50]. Extruded SEBS-g-MA did not show any strong bands at those fingerprint regions, however, two strong peaks were observed at 1735 cm^{-1} and 1715 cm^{-1}. The strong band present at 1715cm^{-1} shows C=O dimers present in COOH dimers [49, 50]. It may be due to the ring opening of MA by hydrolysis phenomenon due to prolong storage of SEBS-g-MA leading to hydrolysis of 95% of Maleic anhydride [49-51]. However, the presence of 1310cm^{-1} -1210 cm^{-1} bands observed by C-O-C stretching of anhydride group suggests that some anhydride groups were still unaltered during extrusion or prolong storage [53]. In addition, observation of 1776cm^{-1} band peak along with other peaks in between 1776cm^{-1} and 1735 cm^{-1} concludes esterification of maleic anhydride due to prolonged storage of SEBS-g-MA elastomer [54]. Moreover, the formation of other groups like alcohol during the process can also be confirmed due to the presence of a strong band at 1045 cm-1 and 1017cm^{-1}[50]. The peak shown at 1601 cm^{-1} confirms the presence of C=C bond of benzene ring [55]

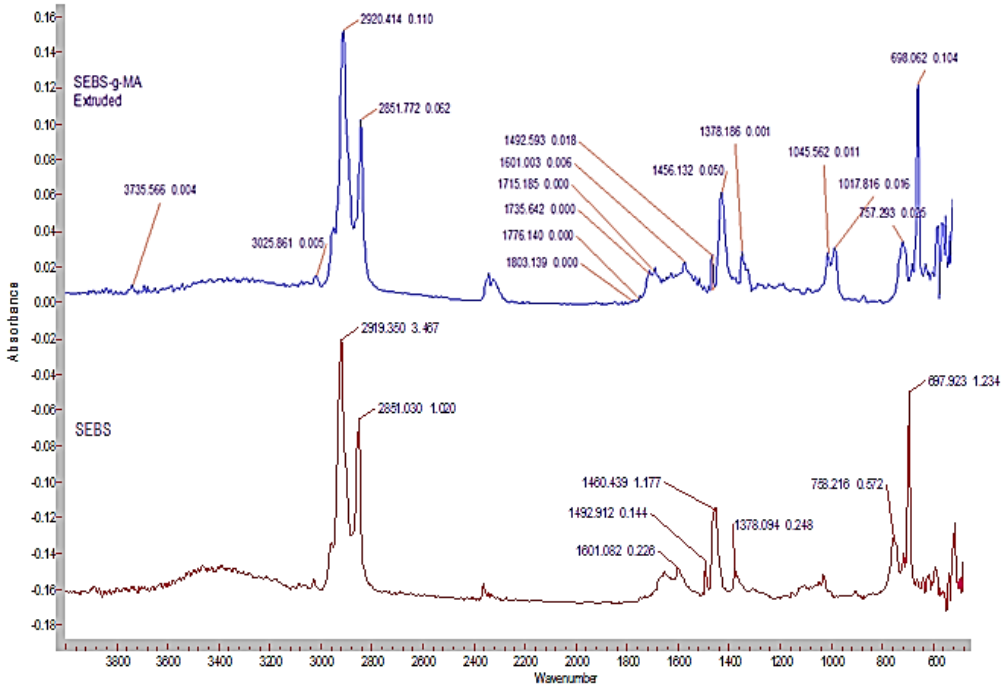

Figure 14 ATR_ FTIR Spectra of SEBS and SEBS-g-MA

Table 6 Different frequency bands of SEBS and SEBS-g-MA observed in FTIR spectra

Wavenumber	Assignment and observations
2919	Asymmetrical stretching vibration of CH_2 in EB units
2851	Symmetrical stretching vibration of CH_2 in EB units
1601, 1492, 1460	Assigned for stretching vibration of carbons in aromatic ring
1715	Assigned for stretching of C=O dimers present in COOH dimers
1378	Wagging of CH_2 in EB units of SEBS
758	Deformation vibration of CH groups in aromatic ring in PS units
697	Out of plan bending of CH groups in aromatic ring in PS units

BT also shows a slight interaction with SEBS thermoplastic elastomers with the C=C of a benzene ring with a change in wavenumber as shown in Figure 15. The intensity of interaction of BT does not change with C=C bond when BT is changed from 5% to 10% (the wavenumber change from 1460 to 1454 cm^{-1} in both cases). In addition, the rocking effect of benzene ring at 758 cm^{-1} wavenumber almost remains constant upon addition of 10% of BT. Figure 16~~Figure 16~~ shows the FTIR graphs of SEBS-g-MA-BT composites. The graphs show BT interacts mainly with Maleic anhydride group. FTIR band shifts and change in intensity, especially in C=O dimmers, C-O-C band peaks, and OH peaks shows the interaction of BT with SEBS-g-MA in acidic or other forms. In addition, change in IR peak band and nature of C=C bond at 1601cm^{-1} also confirms the interaction of benzene ring of polystyrene with BT very slightly. The presence of many other peaks between 1800 cm^{-1} to 1601cm^{-1} confirms a high interaction of BT with MA molecule together with the benzene ring.

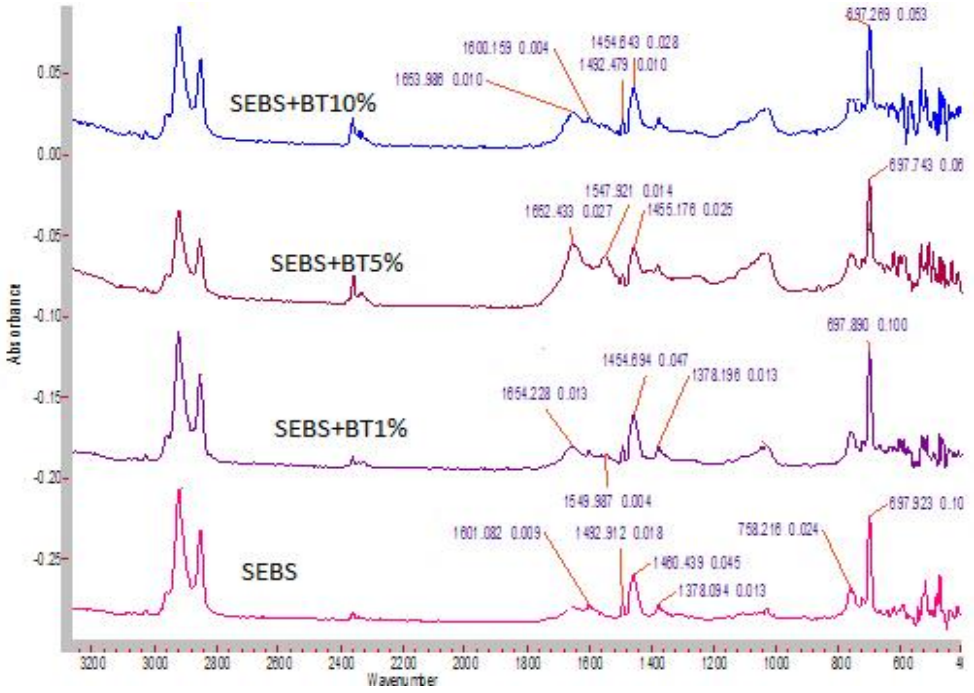

Figure 15 FTIR ~~graphs~~ Spectra of SEBS/BT composites

.

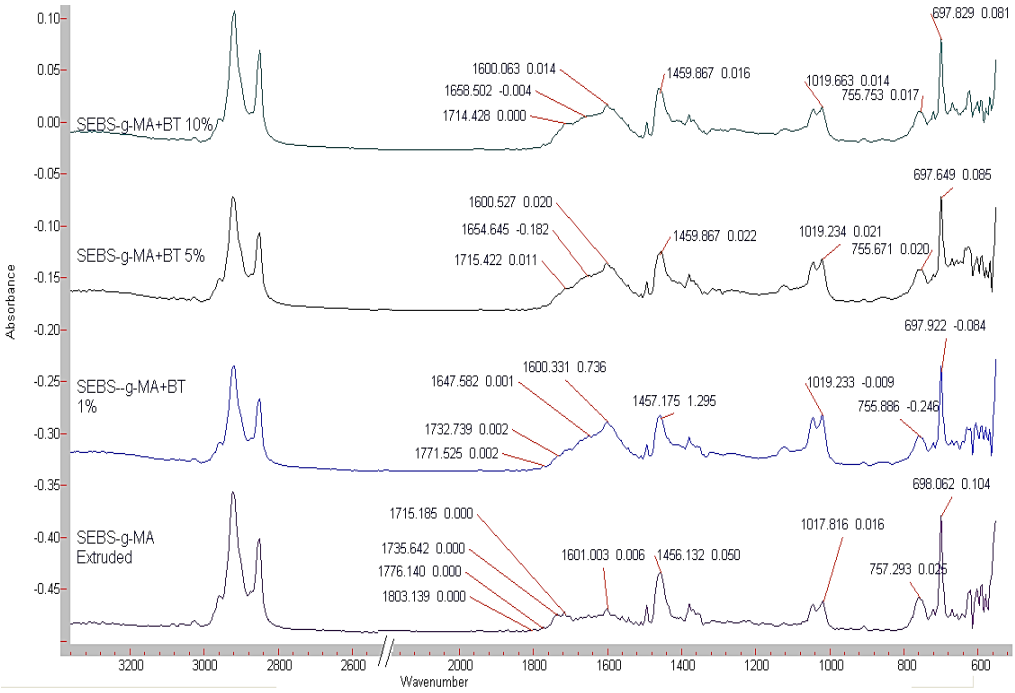

Figure 16 FTIR Spectra of SEBS-g-MA/BT composites

Figure 17~~Figure 17~~(a) and Figure 17~~Figure 17~~(b) show SEM images of SEBS and SEBS-g-MA respectively.

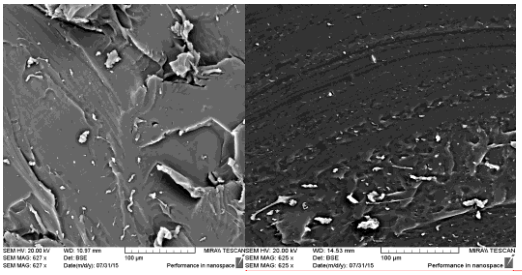

Comment [SL9]: Should make these bigger as they may not reproduce well in the journal at small sizes

Figure 17 SEM images of (a) SEBS left (b) SEBS-g-MA right

Figure 18~~Figure 18~~(a) and Figure 18~~Figure 18~~(b) show SEM images of SEBS and SEBS-g-MA composites. Comparing Figure 17~~Figure 17~~ to Figure 18~~Figure 18~~, the relatively large transformation was observed in SEBS-g-MA nanocomposite than SEBS nanocomposite.

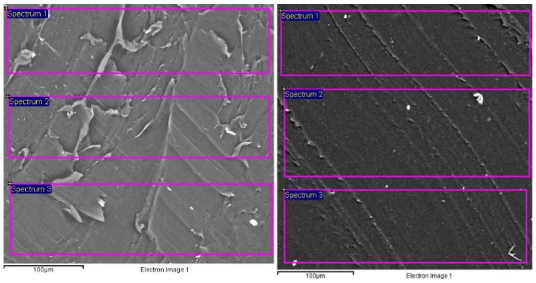

Figure 18 Different spectrum range used for element mapping of (a) SEBS left and (b) SEBS-g-MA Right

For further analysis of dispersion of BT with SEBS and SEBS-g-MA, the element mapping was done along the thickness of each sample as shown in Figure 18~~Figure 18~~

Table 7 Distribution of Ba, Ti, O and C element along different Spectrum on by % weight

Spectrum	SEBS					SEBS-g-MA				
	C	O	Ti	Ba	Total	C	O	Ti	Ba	Total
Spectrum 1	90.50	4.96	1.08	3.46	100.00	90.41	5.19	1.06	3.34	100.00
Spectrum 2	91.15	4.79	0.98	3.09	100.00	90.55	4.97	1.09	3.39	100.00
Spectrum 3	91.39	4.75	0.98	2.89	100.00	90.47	5.01	1.12	3.40	100.00

Mean	91.01	4.83	1.01	3.15	100.00	90.48	5.06	1.09	3.38	100.00
Std. deviation	0.46	0.11	0.06	0.29		0.07	0.12	0.03	0.03	

From Table 7~~Table 7~~, it was observed that the distribution of C, O, Ti and Ba were not uniform along the thickness. The percentage weight of Ba element varies from 3.46 to 2.89 by weight making a wide range of 0.57 and standard deviation of 0.26. Non-uniform dispersion of these elements gave rise to unexpected polarization as well as mechanical behavior during test conditions. Whereas, from Table 7, it can be observed that the dispersion of BT in SEBS-g-MA is uniform with the standard deviation of 0.03 of Ba element. The addition of a polarization group MA in SEBS was found very useful for increasing dielectric as well as compatibility to different polar materials to optimize dielectric and mechanical properties.

From SEM images of SEBS and SEBS-g-MA, BT was found to be poorly distributed along the thickness of a sample for SEBS compared to SEBS-g-MA. Because of poor dispersion of BT in SEBS, SEBS-BT composite samples can be considered as different capacitors with different dielectric constant.

Comment [SL10]: AFM in Waterford – for future work you might get some cool images looking at in phase versus out of phase for these samples

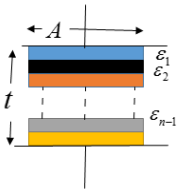

Figure 19 Nanocomposite with poor dispersion of additives

$$1/C = 1/C_1 + 1/C_2 \text{ ----} + 1/C_n \quad (4)$$

$$C = \varepsilon_0 \varepsilon A/t \quad (5)$$

From equation (4) and (5)

$$t/\varepsilon_0\varepsilon A = t_1/\varepsilon_0\varepsilon_1 A_1 + t_2/\varepsilon_0\varepsilon_2 A_2 \ldots\ldots\ldots + t_n/\varepsilon_0\varepsilon_n A_n \quad (6)$$

Where, $\varepsilon_1, \varepsilon_2 \ldots\ldots\ldots\ldots \varepsilon_n$,correspond to the dielectric permittivity existed along the sample of capacitance $C_1, C_2 \ldots\ldots C_n$ with thickness $t_1, t_2 \ldots\ldots t_n$ and cross section area $A_1, A_2 \ldots\ldots A_2$ respectively due to poor dispersion of nanofillers into the polymer matrix. For simplicity, thickness and cross section area was considered to be constant for all small capacitors existed within a sample thickness.

Then, then equation (6) reduces to equation (7)

$$1/\varepsilon = 1/n(1/\varepsilon_1 + 1/\varepsilon_2 ..... + 1/\varepsilon_n) \qquad (7)$$

If we consider three small capacitors with dielectric permittivity with 2, 5, and 10 arranged in parallel as shown in Figure 19~~Figure 19~~, then the average- dielectric permittivity measured by an instrument is valued at 3.5 only. But, as the dispersion level increases, the dielectric permittivity of all small capacitor becomes almost the same causing an increase in overall dielectric permittivity of composites. This theory is not valid on samples with very small thickness as the dispersion level does not vary so much even nanocomposites are non-compatible.

Comment [SL11]: What thicknesses?

Comment [SL12]: End of sentence doesn't really make sense

4 Conclusions

Polarization enhancements with very low dielectric loss were achieved on non-polarizing (SEBS) copolymers and polarizing copolymers (SEBS-g-MA) using a different concentration of dielectric filler materials (BT) by using a co-rotating twin screw extrusion system. However, the compatibility and interaction between polymers and additive were found to be crucial for increasing polarization as well as to obtained better mechanical properties. FTIR, DSC, and DMA results showed the high interaction of BT with SEBS-g-MA compared to SEBS leading to the high dispersion of BT in SEBS-g-MA than SEBS polymer matrix. Change in heat enthalpy and rearrangement of micro-molecules upon BT addition on different polymer matrices had led to different thermal, electrical, morphological and mechanical behaviors. However, no significant change in the glass transition of polymer matrix was observed upon addition of BT in all composite type.

The high increase in dielectric permittivity with the low dielectric loss with minimum change in loss factor was observed on SEBS-g-MA, this result suggests the potential of these manufactured nanocomposites can be used not for stress and strain sensors, robotic artificial muscles applications but also for capacity energy harvesters and charge storing devices.

Minimum change in mechanical properties (Young's modulus, resilience as well as stiffness in both transverse as well as parallel to extrusion) compared to the high change in dielectric permittivity also suggest that SEBS-g-MA- BT nanocomposites manufactured using this technology are highly sensitive to compression force as well as posse high Maxwell stress under an electric field. Moreover, from DMA and DSC analysis, it can be suggested that temperature plays a major role in defining the structural, and mechanical changes of nanocomposites. The continuous decrease in storage modulus over temperature well as a change in heat enthalpy over a range of temperature suggests the continuous changes in microphase domains in SEBS and SEBS-g-MA nanocomposites even in a small change in temperature resulting different electromechanical response over temperature.

5 Acknowledgements

The authors wish to acknowledge the Waterford Institute of Technology Ph.D. scholarship program for financial support. Special thanks to South Eastern Applied Materials Research Centre (SEAM), WIT and the Applied Polymer Technology Research Centre, AIT for their support throughout the work.

6 References

[1] Kim B, Park YD, Min K, Lee JH, Hwang SS, Hong SM, et al. Electric Actuation of Nanostructured Thermoplastic Elastomer Gels with Ultralarge Electrostriction Coeffi cients. Adv Funct Mater. 2011;21(17):1-8.
[2] Rajagopalan M, Jeo i-H, Oh I-K. Electric-stimuli-responsive bending actuator based on sulfonated polyetherimide. Sensors and Actuators B: Chemical. 2010;151(1):198–204.
[3] Okuzaki H, Takagi S, Hishiki F, Tanigawa R. Ionic liquid/polyurethane/PEDOT: PSS composites for electro-active polymer actuators. Sensors and Actuators B: Chemical. 2014;194:59-63.
[4] Chen T, Pan L, Lin M, Wang B, Liu L, Li Y, et al. Dielectric, mechanical and electro-stimulus response properties studies of polyurethane dielectric elastomer modified by carbon nanotube-graphene nanosheet hybrid fillers. Polymer Testing. 2015;47:4-11.
[5] Kear KE. Structure of Thermoplastic Elastomers. Developments in Thermoplastic Elastomers: Smithers Rapra; 2003. p. 3-6.
[6] Chatterjee K, Naskar K. Development of thermoplastic elastomers based on maleated ethylene propylene rubber (m-EPM) and polypropylene (PP) by dynamic vulcanization. Express Polym Lett. 2007;1:527-34.
[7] Stoyanov H. Soft nanocomposites with enhanced electromechanical response for dielectric elastomer actuators [Doctoral Thesis]. Patsdam: University of Potsdam; 2011.
[8] Shankar R, Ghosh TK, Spontak RJ. Electroactive Nanostructured Polymers as Tunable Actuators. Adv Mater. 2007;19:2218–23.
[9] Pelrine R, Kornbluh R, Joseph J, Heydt R, Pei Q, Chiba S. High-field deformation of elastomeric dielectrics for actuators. Materials Science and Engineering: C. 2000;11(2):89-100.
[10] Pelrine R, Kornbluh R, Pei Q, Joseph J. High-speed electrically actuated elastomers with strain greater than 100%. Science. 2000;287(5454):836-9.
[11] Koo CM. Electroactive Thermoplastic Dielectric Elastomers as a New Generation Polymer Actuators: INTECH Open Access Publisher; 2012.
[12] Chen L, Wang X, Zhang X, Zhang H. 3D porous and redox-active prussian blue-in-graphene aerogels for highly efficient electrochemical detection of H 2 O 2. Journal of Materials Chemistry. 2012;22(41):22090-6.
[13] Nelson SO. Fundamentals of dielectric properties measurements and agricultural applications. Journal of Microwave power and electromagnetic energy. 2010;44(2):98-113.
[14] Mannsfeld SC, Tee BC, Stoltenberg RM, Chen CVH, Barman S, Muir BV, et al. Highly sensitive flexible pressure sensors with microstructured rubber dielectric layers. Nature materials. 2010;9(10):859-64.
[15] Houqlng Z, Jlanguo L, Xmrong W, Yanhong X, Hongping Z. Applications of Terfenol-D in China. Journal of Alloys and Compounds. 1997;258(1-2):49-52.
[16] Olabi A-G, Grunwald A. Design and application of magnetostrictive materials. Materials & Design. 2008; 29(2):469-83.
[17] Shankar R, Ghosh TK, Spontak RJ. Electromechanical Response of Nanostructured Polymer Systems with no Mechanical Pre-Strain. Macromolecular rapid communication. 2007;28:1142–7.
[18] Brochu P, Pei Q. Advances in Dielectric Elastomers for Actuators and Artificial Muscles. Macromolecular Rapid Communications. 2010;31(1):10-36.
[19] Ranjan V, Yu L, Nardelli MB, Bernholc J. Phase equilibria in high energy density PVDF-based polymers. Physical review letters. 2007;99(4-27):047801.
[20] Poudel A, Coffey A, Kennedy J, Lyons S, Thomas K, Walsh P. Dielectric Polarization Enhancement of Thermoplastic Elastomers for Sensing and Energy Harvesting Applications. International Journal of Materials, Mechanics and Manufacturing. 2016;4(4):237-42.
[21] He L, Tjong SC. Low percolation threshold of graphene/polymer composites prepared by solvothermal reduction of graphene oxide in the polymer solution. Nanoscale research letters. 2013;8(1):1.
[22] Wang Z, Nelson JK, Miao J, Linhardt RJ, Schadler LS, Hillborg H, et al. Effect of high aspect ratio filler on dielectric properties of polymer composites: a study on barium titanate fibers and graphene platelets. Dielectrics and Electrical Insulation, IEEE Transactions on. 2012;19(3):960-7.

[23] Kim MH, Hong SM, Koo CM. Electric actuation properties of SEBS/CB and SEBS/SWCNT nanocomposite films with different conductive fillers. Macromolecular Research. 2012;20(1):59-65.
[24] Hourston DJ, Song M, Hammiche A, Pollock HM, Reading M. Modulated differential scanning calorimetry: 6. Thermal characterization of multicomponent polymers and interfaces. Polymer. 1997;38(1):1-7.
[25] Donth EJ. Relaxation and Thermodynamics in Polymers: Glass Transition: Wiley; 1993.
[26] Zhang Z-F, Bai X-F, Zha J-W, Li W-K, Dang Z-M. Preparation and dielectric properties of BaTiO3/epoxy nanocomposites for embedded capacitor application. Composites Science and Technology. 2014;97(0):100-5.
[27] Heaney MB. Measurement and interpretation of nonuniversal critical exponents in disordered conductor–insulator composites. Physical Review B. 1995;52(17):12477.
[28] Sau K, Chaki T, Khastgir D. Conductive rubber composites from different blends of ethylene-propylene-diene rubber and nitrile rubber. Journal of materials science. 1997;32(21):5717-24.
[29] Achour ME, Brosseau C, Carmona F. Dielectric relaxation in carbon black-epoxy composite materials. Journal of Applied Physics. 2008;103(9):094103.
[30] El Hasnaoui M, Triki A, Achour ME, Arous M. Modelling of dielectric relaxation processes of epoxy-resin filled with carbon black particles. Physica B: Condensed Matter. 2014;433(0):62-6.
[31] El Hasnaoui M, Belattar J, Achour M, Costa L, Lahjomri F. Electrical transport properties of CB/epoxy polymer composites. Optoelectron Adv Mater-Rapid Commun. 2012;6:610-3.
[32] Patsidis A, Kalaitzidou K, Psarras G. Dielectric response, functionality and energy storage in epoxy nanocomposites: Barium titanate vs exfoliated graphite nanoplatelets. Materials Chemistry and Physics. 2012;135(2):798-805.
[33] Yang T-I, Kofinas P. Dielectric properties of polymer nanoparticle composites. Polymer. 2007;48(3):791-8.
[34] Roylance D. Stress-strain curves. Massachusetts Institute of Technology study, Cambridge. 2001.
[35] Cantournet S, Desmorat R, Besson J. Mullins effect and cyclic stress softening of filled elastomers by internal sliding and friction thermodynamics model. International Journal of Solids and Structures. 2009;46(11):2255-64.
[36] Mullins L. Effect of stretching on the properties of rubber. Rubber Chemistry and Technology. 1948;21(2):281-300.
[37] Wang Z, Pinnavaia TJ. Nanolayer reinforcement of elastomeric polyurethane. Chemistry of Materials. 1998;10(12):3769-71.
[38] Kohls D, Beaucage G. Rational design of reinforced rubber. Current opinion in solid state and materials science. 2002;6(3):183-94.
[39] Sauceau M, Fages J, Common A, Nikitine C, Rodier E. New challenges in polymer foaming: a review of extrusion processes assisted by supercritical carbon dioxide. Progress in Polymer Science. 2011;36(6):749-66.
[40] Karanth H, Shenoy VS, Murthy RR. Industrially feasible alternative approaches in the manufacture of solid dispersions: a technical report. AAPS PharmSciTech. 2006;7(4):E31-E8.
[41] Elkovitch MD, Tomasko DL. Effect of supercritical carbon dioxide on morphology development during polymer blending. Polymer Engineering & Science. 2000;40(8):1850-61.
[42] Kazarian S. Polymer processing with supercritical fluids. Polymer Science Series CC/C of Vysokomolekuliarnye Soedineniia. 2000;42(1):78-101.
[43] Klempner D. Advances in interpenetrating polymer networks: CRC Press; 1994.
[44] Tsagaropoulos G, Eisenberg A. Dynamic mechanical study of the factors affecting the two glass transition behavior of filled polymers. Similarities and differences with random ionomers. Macromolecules. 1995;28(18):6067-77.
[45] Robertson CG, Lin C, Rackaitis M, Roland C. Influence of particle size and polymer− filler coupling on viscoelastic glass transition of particle-reinforced polymers. Macromolecules. 2008;41(7):2727-31.
[46] Payne AR. The dynamic properties of carbon black-loaded natural rubber vulcanizates. Part I. Journal of Applied Polymer Science. 1962;6(19):57-63.
[47] Cassagnau P. Payne effect and shear elasticity of silica-filled polymers in concentrated solutions and in molten state. Polymer. 2003;44(8):2455-62.
[48] Tananuwong K, Reid DS. Differential scanning calorimetry study of glass transition in frozen starch gels. Journal of agricultural and food chemistry. 2004;52(13):4308-17.
[49] Liu R, Farinha J, Winnik M. Preparation and spectroscopic properties of phenanthrene-labeled SEBS triblock copolymers. Macromolecules. 1999;32(12):3957-63.
[50] Stuart BH. Infrared Spectroscopy: Fundamentals and Applications: Wiley; 2004.
[51] BALKAN O, DEMİRER H, EZDEŞİR A, YILDIRIM H, YILMAZER Ü. EFFECTS OF SEBS AND SEBS-g-MA MODIFICATIONS ON THE FRACTURE BEHAVIOR OF i-PP/GLASS BEAD AND i-PP/WOLLASTONITE COMPOSITES.
[52] Munteanu S, Vasile C. Spectral and thermal characterization of styrene-butadiene copolymers with different architectures. Journal of Optoelectronics and Advanced materials. 2005;7(6):3135.

[53] Kwee T, Mauritz KA, Beyer F. Poly [styrene-b-maleated (ethylene/butylene)-b-styrene](mSEBS) block copolymers and mSEBS/inorganic nanocomposites: I. Morphology and FTIR characterization. Polymer. 2005;46(11):3871-83.
[54] Pracella M, Haque MM-U, Alvarez V. Functionalization, compatibilization and properties of polyolefin composites with natural fibers. Polymers. 2010;2(4):554-74.
[55] Cao Y, Lai Z, Feng J, Wu P. Graphene oxide sheets covalently functionalized with block copolymers via click chemistry as reinforcing fillers. Journal of Materials Chemistry. 2011;21(25):9271-8.

7 Figure Captions

8 List of Tables